UJEAS

UNIZIK JOURNAL OF ENGINEERING AND APPLIED SCIENCES

UNIZIK Journal of Engineering and Applied Sciences 5(3), September (2025), 2758-2770
Journal homepage: https://journals.unizik.edu.ng/index.php/ujeas
PRINT ISSN: 2992-4383 || ONLINE ISSN: 2992-4391

Phyto-chemical screening, proximate analysis mineral composition of *musa paradisiaca* leaf ash (MPLA) for water treatment applications

Nwankwo I.H[1*]. and Nwaiwu N.E.[2]
Department of Civil Engineering, Nnamdi Azikwe University Awka, Anambra State Nigeria.
*Corresponding author email: nifeanyihenry@yahoo.com

Abstract
The pervasive issue of accessing potable water remains a critical challenge in numerous developing nations, conventional water treatment methodologies frequently rely on synthetic chemicals, which often necessitate importation at considerable expense, potential health risks, exemplified by the correlation between aluminum-based coagulants and the onset of Alzheimer's disease, the production of substantial sludge volumes. Consequently, the imperative to mitigate the risks inherent in synthetic chemical usage necessitates the exploration of cost-effective and sustainable alternatives for water treatment, without compromising coagulation efficacy or microbiological integrity. Natural coagulants present an environmentally conscious alternative to their chemical counterparts. *Musa Paradisiaca* leaf ash is an agricultural waste in need of disposal. In this work the characterization of *Musa paradisiaca* leaf ash was undertaken to investigate suitability for water treatment applications. The results reveal the existence of Aluminium (AI) 12.3%, 7.5%, Carbon (C) 7.0%, 6.67%, Calcium (Ca) 5.20%, 22.09%, Iron, (Fe) 3.0%, 5.0%, Nitrogen (N) 4.0%, 4.0%, Oxygen (O) 20.3%, 10.43%, and Silicon (Si) 47.3%, 44.31% for *Musa paradisiaca* leaf ash and *Musa paradisiaca* stalk ash respectively. The result for nutritional content are as follows 1.95 mg/100g and 2.35 mg/100g for tannin, 0.16 mg/100g and 0.19 mg/100g for phytate, 0.48 mg/100g and 1.72 mg/100g for alkaloid, 8.7 mg/100g and 2.7 mg/100g for saponin, 36.55 mg/100g and 38.14 mg/100g for flavonoid, 18.6 mg/100g and 2.1 mg/100g for crude protein 9.5 mg/100 and 9.6 mg/100g for moisture content, 7.3 mg/100g and 9.2 mg/100g for ash content, 54.4 mg/100g and 63.5 mg/100g for carbohydrate, 1.6 mg/100g and 0.9 mg/100g for crude lipids and 8.6 mg/100g and 14.7 mg/100g for crude fibre for Musa paradisiaca leaf ash and Musa paradisiaca Stalk ash respectively.
Keywords: Musa Paradisiaca, Proximate Analysis, Water treatment, Coagulation, Flocculation.

1. Introduction

Water treatment is an indispensable process in public drinking water systems, employing a variety of methods to ensure the delivery of safe and potable water to communities, with the specific treatment approach tailored to the unique characteristics of the raw water source entering the treatment plant (Ratnaweera, 2020). This treatment encompasses a range of interventions designed to enhance the suitability of water for specific end uses, spanning from drinking and industrial applications to irrigation and the maintenance of river flow, as well as the safe return of water to the environment (Kurniawan, Abdullah, Imron, etal., 2020). The primary objective of water treatment is to eliminate contaminants or reduce their concentration, thereby rendering the water appropriate for its intended purpose (Shan, 2019). Surface runoff water, often utilized for household purposes, carries a multitude of impurities, including silt particles, solids, bacteria, and other microorganisms, some of which are pathogenic, necessitating their removal before the water can be deemed safe for human consumption (Futi, Otieno, Acholla, Otieno, Ochieng and Mukisira, 2011, Kumar, Qureshi, Vishwakarma *etal*., 2022). Factors such as population growth and economic development contribute to elevated pollutant concentrations in water bodies. Consequently, water must undergo a series of treatments to guarantee its safety and freedom from contamination (Alprol Mansour, Ibrahim, and Ashour. 2024; Azman and Adenan 2019; Lv, Zhang, Zeng, Lui *et al*., 2019; Mungondori, Muchingami, Taziwa and Chaukura, 2021; Wang and Yang 2016; Zhao, Xu, Lui, Wang, Zhao *et al*., 2018).

Coagulation and flocculation stand out as critical processes for the removal of smaller or colloidal suspended particles from surface water, which are responsible for turbidity (Rahman, Ahmed, Khan. and Joy, 2016; Srinivasan, 2011). Coagulation is a widely employed technology in water treatment (Jiang, 2015). Coagulation is the process of

destabilizing the collides, suspended substances and other organic matter by adding coagulants to the liquids and allowing them to be converted into a bigger form that is easier to removed (Khader, Mohammed and Mirghaffari, 2018; Odika, Nwansiobi, Nwankwo, Ekwunife and Onuoha, 2020). Natural coagulants are naturally occurred plants based, animal or micro-organism coagulants that can be used in coagulation-flocculation process of water/wastewater treatment for reducing turbidity (Karanja, Fengting and Nganga, 2017; Saravanan, Priyadharshini, Soundammal, Sudha and Suriyakala, 2017; Venkata, Ramamohan, and Rao, 2017). The use of natural coagulants from plant origin to clarify turbid raw water is not a new idea (Iqbal, Hussain, Haydars and Zahara, 2017; Jayalakshmi, Bhanya and Saritha, 2016). Natural coagulants are eco-friendly methods albio-fertilizer (Sasikala and Muthuraman, 2017). They are sustainable environmental technology used in removal of turbidity from water and are mainly used in some less developed communities due to its relatively cost effective compared to chemical coagulants and are easily biodegradable (Sasikala and Muthuraman 2017). The aim of this research work is to determine the proximate and phyto-chemical analysis of *Musa paradisiaca* leaf ash (MpLA).

2. Materials and Methods

2.1 Harvesting of *Musa paradisiaca* leaf

Freshly dried *Musa paradisiaca* leaves were harvested from local farms located in Nsukka, 9th Mile Corner, and Emene all in Enugu State, Nigeria. The leaves were sent to the Department of Crop Science, Nnamdi Azikiwe University, for botanical identification. After confirmation, the harvested leaves were thoroughly washed with distilled water to remove surface impurities and subsequently sun-dried for 30 days. The dried leaves were then stored in a clean, white container before being transported to the Scientific Equipment Development Institute (SEDI), Enugu, for processing into ash.

2.2 Proximate analysis of *Musa paradisiaca* ash (MLA)

2.2.1 Determination of moisture content

1.0 g of the *Musa paradisiaca* ash (MLA) was collected and dried in an oven at 150 °C for four hours, until the weight of the sample became constant. The difference in mass represented the amount of moisture content adsorbed (Dada, Olalekan, Oletanya and Dada, 2012). The moisture content was determined using Equation (1).

$$Moisture\ Content\ (\%) = 100\frac{(B-A)-(C-A)}{(B-A)} \quad (1)$$

Where

A is weight of clean, dry scale pan (g)
B is weight of scale pan + wet sample (g)
C is weight of scale pan + dry sample (g)

2.2.2 Determination of adsorbent pH

The pH of the adsorbent was determined using the standard test method for the determination of pH of *Musa paradisiaca* ash (MLA) in accordance with ASTM D3838-80. A 1.0 g sample of MLA was weighed and transferred into a beaker. Then, 100 mL of distilled water was measured and added to the pre-weighed MLA, and the mixture was stirred for one hour. The resulting solution was allowed to stabilize before the pH was measured using a pH meter.

2.2.3 Determination of percentage ash content

A 5 g sample of dry *Musa paradisiaca* ash (MLA) was placed in a crucible that had been previously calcined and brought to constant weight. The crucible was then placed in a furnace and heated at 550 °C for 12 hours. After heating, it was allowed to cool and subsequently transferred to a desiccator. The crucible, now containing the ash, was carefully weighed again (Hirp, Nigussie-Dechassa, Setega and Bultosa, 2015). The ash content was determined using Equation (2).

$$Ash\ content\ (\%) = 100\frac{A-B}{C} \quad (2)$$

Where A is weight of crucible with sample (g), B is weight of crucible with ash (g), C is weight of sample (g)

2.2.4 Fourier transform infrared spectroscopy (FTIR) analysis

A 1 mg sample was ground and mixed with 100 mg of potassium bromide (KBr) to form a fine powder. The mixture was then compressed into a thin pellet under a pressure of 7 tons for 5 minutes. The sample was analyzed using a Shimadzu 8300 FTIR spectrometer, and the spectrum was recorded in the mid-infrared (mid-IR) range from 4000 to 400 cm^{-1}, with a resolution of 1 cm^{-1}.

2.2.5 Scanning electron microscopy (SEM)

To study the effect of activation on porosity and to observe the surface physical morphology of *Musa paradisiaca* ash (MLA), Scanning Electron Microscopy (SEM) was employed (Aji, Gutti and Highina, 2015). The scanning electron micrographs enabled direct observation of the surface microstructures of the adsorbent (Ahamed, Chandrasekaran and Kumar, 2013). Surface morphology was examined using a JEOL JSM-5600LV scanning electron microscope, and images were recorded without sample coating. The surface area was estimated by agitating 1.5 g of MLA in 100 mL of diluted hydrochloric acid adjusted to a pH of 3. Subsequently, 30 g of sodium chloride was added while stirring the suspension, and the total volume was brought up to 150 mL using deionized water. The resulting solution was titrated with 0.10 N NaOH to raise the pH from 4 to 9, and the volume of NaOH used was recorded.

2.3 Phyto-chemical Screening of *Musa paradisiaca* Ash (MLA):

2.3.1 Determination of saponin

Five grams (5 g) of *Musa paradisiaca* leaf ash (MLA) was measured into a 250 mL beaker containing 20% v/v acetic acid in ethanol. The mixture was allowed to stand in a water bath at 50 °C for 24 hours. After extraction, the solution was filtered, and the filtrate was concentrated to one-quarter of its original volume using a water bath. Concentrated ammonium hydroxide (NH_4OH) was then added dropwise to the concentrated extract until complete precipitation occurred. The entire mixture was allowed to settle, and the precipitate was collected by filtration and weighed. The percentage saponin content was calculated using Equation (3) (Oluduro and Aderiye, 2007).

$$\%\ saponin\ content = \frac{weight\ of\ filter\ paper + residue(g) - weight\ of\ filter\ paper\ (g) \times 100}{weight\ of\ sample\ analyzed\ (g)} \quad (3)$$

2.3.2 Determination of alkaloids

The alkaloid content was determined using the procedure described by Oluduro and Aderiye (2007). Five grams (5 g) of *Musa paradisiaca* leaf ash (MLA) was weighed into a 250 mL beaker, and 200 mL of acetic acid in ethanol was added. The beaker was covered, and the contents were allowed to stand for four (4) hours at 25 °C. The mixture was then filtered using Whatman filter paper, and the filtrate was concentrated to one-quarter of its original volume using a water bath (Model 121, WB-12).

Concentrated ammonium hydroxide (NH_4OH) was added to the extract until complete precipitation occurred. The mixture was allowed to settle, and the resulting precipitate was collected and washed with dilute ammonium hydroxide (1% NH_4OH solution). The residue was filtered using Whatman filter paper and then dried in an oven at 80 °C.
The alkaloid content was calculated and expressed as a percentage using Equation (4).

$$\%\ weight\ of\ alkaloid = \frac{weight\ of\ filter\ paper + residue - weight\ of\ filter\ paper\ \times 100}{weight\ of\ sample\ analyzed} \quad (4)$$

2.3.3 Determination of tannin

Tannin content was determined using the Folin-Denis titration method according to the procedure described by Pearson (1976). Twenty grams (20 g) of *Musa paradisiaca* leaf ash (MLA) was measured into a conical flask and mixed with 100 mL of petroleum ether. The flask was covered and left to stand for 24 hours. The sample was then filtered and allowed to stand for 15 minutes to enable evaporation of the petroleum ether.
Subsequently, the residue was re-extracted by soaking in 100 mL of 10% acetic acid in ethanol for four (4) hours. The mixture was filtered, and the filtrate collected. To precipitate the alkaloids, 25 mL of ammonium hydroxide (NH_4OH) was added to the filtrate. After precipitation, the mixture was heated on an electric hot plate to concentrate the solution. Five milliliters (5 mL) of the concentrated solution was transferred into a beaker containing 20 mL of ethanol. The mixture was then titrated with 0.1 M NaOH using phenolphthalein as an indicator until a pink endpoint was reached. The percentage tannin content was calculated using Equations (5) and (6).

$$\%\ of\ tannic\ acid\ content = \frac{C_1}{weight\ of\ sample\ analyzed\ (g)} \quad (5)$$

$$C_1 = \frac{C_2 V_2}{V_1} \quad (6)$$

Where
C_1 = Concentration of tannic acid,
C_2 = Concentration of the base,
V_1 = Volume of the tannic acid and
V_2 = Volume of the base.

2.3.4 Determination of phytate

The phytate content was determined using the method described by Peter, Robert, Mokgalaka, and McCrindle (2011) following the procedure below. A 0.2 g sample of *Musa paradisiaca* leaf ash (MLA) was weighed into a 250 mL conical flask and soaked in 100 mL of 2% hydrochloric acid (HCl) for 3 hours, then filtered.
Fifty milliliters (50 mL) of the filtrate was transferred into a 250 mL beaker, and 100 mL of distilled water was added. The solution was titrated with a standard iron (III) chloride ($FeCl_3$) solution (containing 0.00195 g iron per mL) using 10 mL of 0.3% ammonium thiocyanate solution as an indicator.
The phytate content was calculated using Equation (7).

$$Percentage\ (\%)\ of\ Phytate\ content = \frac{Titre\ value\ \times 0.00195 \times 19 \times 100}{weight\ of\ the\ sample\ (g)} \quad (7)$$

2.3.5 Determination of flavonoids

Five grams (5 g) of *Musa paradisiaca* leaf ash (MLA) sample was extracted separately with 50 mL of 80% aqueous methanol in triplicate at room temperature. The entire solution was filtered through Whatman filter paper No. 42 (125 mm). The filtrate was transferred into a 200 mL beaker and evaporated to dryness over a water bath. The weight of the residue was measured, and the percentage flavonoid content was calculated (Aborishade, Adetutu and Owoade, 2017; Arulpriya and Lalitha, 2013). The percentage of flavonoid concentration was calculated using Equation (8).

$$\%\ weight\ of\ flavonoids = \frac{(weight\ of\ crucible + residue\ ) - (weight\ of\ crucible) \times 100}{weight\ of\ sample\ analyzed} \quad (8)$$

2.3.6 Crude protein

The crude protein of *Musa Paradisiaca* leaf ash was determined by the Kjedahl method. 0.5 g of *Musa Paradisiaca* leaf ash was mixed with 10 ml of concentrated sulphuric acid (H2SO4) in a Kjeldahl digestion flask. A tablet of selenium catalyst was added to it and the mixture was digested by heating under a fume cupboard until a clear solution was obtained. Each of the digest was carefully transferred into a 100 ml volumetric flask and made up to the mark with distilled water. A 10 ml portion of each digest was mixed with an equal volume of 45% NaOH solution in a Kjeldahl distilling unit. The mixture was distilled and the distillate collected into 10 ml of 4% butyric acid solution containing three (3) drops of mixed indicator, bromocressol green and methyl red. 50 ml of the distillate was collected and titrated against 0.02 N H2SO4 solution until it changed from green to a deep red end point. A reagent blank was also digested, distilled and titrated, just as the sample. The total nitrogen thus determined was multiplied by the factor 6.38 to obtain the protein content.

2.3.7 Crude fibre

Five grams (5 g) of *Musa paradisiaca* leaf ash was defatted, and the defatted sample was boiled in 200 mL of 1.25% sulfuric acid (H_2SO_4) solution under reflux for thirty minutes. After boiling, the sample was washed thoroughly with hot water using a double-layer muslin cloth to trap the particles. The washed sample was carefully transferred into a pre-weighed porcelain crucible, dried in an oven at 105 °C for one hour, cooled in a desiccator, and reweighed. The loss in weight after drying was calculated as the crude fiber content and expressed as a percentage of the original sample weight.

3. Results and Discussions.

3.1 Chemical Characteristics of *Musa paradisiaca Leaf Ash* (MLA)

3.1.1 Fourier transform infrared spectroscopy (FTIR) of *Musa paradisiaca leaf ash* (MLA).

Fourier transform infrared spectroscopy (FTIR) was carried out in order to identify the functional groups present in the *Musa paradisiaca* Leaf Ash, stalk (MLA), Figures 1 and 2 and Tables 1 and 2 shows the functional group and surface properties of the coagulants and absorbents by FTIR spectra. Functional groups of adsorbents affect the

adsorption behaviors and also dominates the adsorption mechanism of *Musa paradisiaca leaf ash* (MLA) (Akpomie, Conradie, Adegoke, Oyedotun, Ighalo and Amaku, et al., 2023; Alsawy, Rashad, EL-Qelish, and Mohammed, 2022; Deng, Shao, Ren, Hou, Tang and Hursthouse, 2019; Jiang, Chen, Wang, LV, Dai, and Zhang, et al., 2022; Liang, Cao, Liu, Zeb, Cui and Sun. 2020; Wang, Wang, Zhou and Gao, 2023; Xu, Qu, Yang, Qu, Shan and Yan, *et al*., 2022; Yang, Wan, Zheng, He, Yu, Huang, *et al*., 2019; Zhang and Wu, 2022).

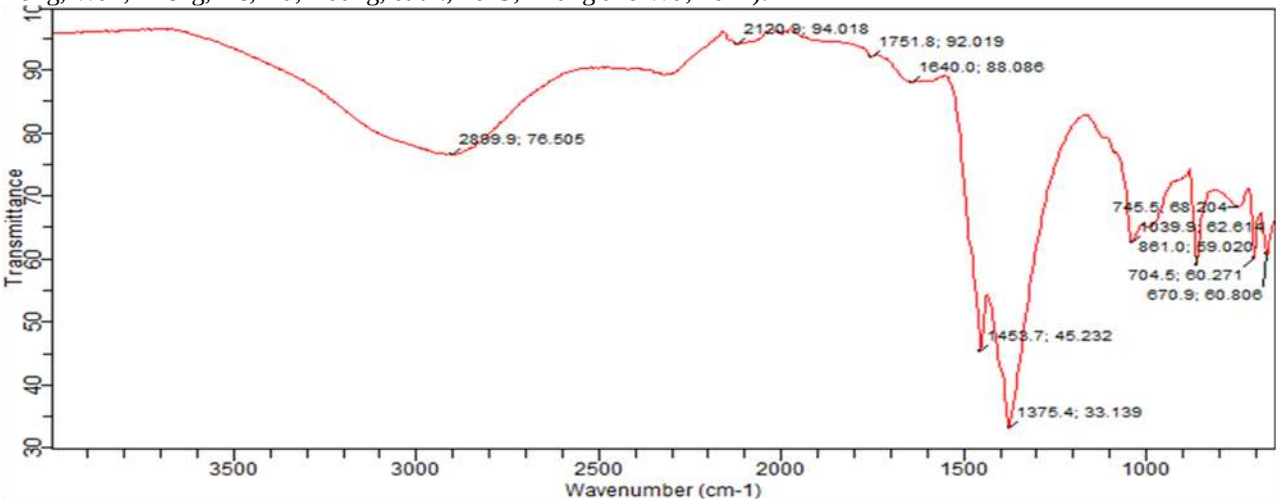

Fig. 1: Fourier Transform Infrared Spectroscopy (FTIR) of Musa paradisiaca leaf Ash (MLA).

The spectra of the Musa paradisiaca Leaf Ash (MLA) used as coagulants was measured in the range of 4000 cm-1 to 650 cm1 wave number. The FT-IR spectrum reveals the complex nature of the coagulants as evidence by the presence of large number of peaks (Karnena and Saritha, 2022; Newman and Cragg, 2020; Peets, Kaupmees, Vahur and Lerto, 2019). The band in the region of 2889.9 cm^{-1} indicates the presence of methyne C-H stretch, lipids/fatty acids and also CH_2/CH_3 groups in carbohydrates chains (starch/cellulose), the band at 2120.9 cm^{-1} correspond to C≡C terminal alkyne which relates to presences of cyanide and thiocyanate ions, the band at 1751.8 cm^{-1} was due to alkyl carbonate in *Musa paradisiaca* this commonly indicates esterified pectin's (methyl esters in pectin) or lipid esters, pectin can adsorb onto particles and form bridges that agglomerate fine colloids into settleable flocs. the band at 1640 cm^{-1} corresponds to alkenyl C=C stretch and indicates the presences of open chain amino (-C=N-), this region often contains overlapping contributions from water bending, proteins (amide 1) and conjugated C=O in polyphenols.

Table 1:Fourier Transform Infrared Spectroscopy (FTIR) of Musa paradisiaca leaf Ash (MLA).

S/N	Peaks (cm^{-1})	Functional group
1	2889.9	Methyne C-H Stretch
2	2120.9	C-=C terminal alKyne (Monosubstituted)
3	1751.8	Alkyl carbonate
4	1640	Alkenyl c=c stretch
5	1453.7	Methylene C-H bend
6	1375.4	Methylene C-H bend
7	1039.9	cyclohexane ring vibrations
8	861	skeletal c-c vibrations
9	745.5	skeletal c-c vibrations
10	704.5	skeletal c-c vibrations
11	670.9	Alkyne C-H bend

The band at 1453.7 cm^{-1} can be ascribed to methylene C-H bend typical of carbohydrates and lipids, the band at 1375.4 cm^{-1} corresponds to methylene C-H bend and indicates presences of aliphatic nitro compounds, the band at 1039.9 cm^{-1} indicates cyclohexane ring vibrations, the band at 861 cm^{-1}, 745.5 cm^{-1} and 704.5 cm^{-1} indicates skeletal C-C vibrations while the band at 670.9 cm^{-1} reveals presences of alkyne C-H bend, suggests some aromatic compounds example traces of lignin or phenolic constituents which aid adsorption of some contaminants (Akinyemi, Akinbomi and Abbey, 2020; Venegas, Torres, Rueda, Morales, Arias and Porras, 2022).

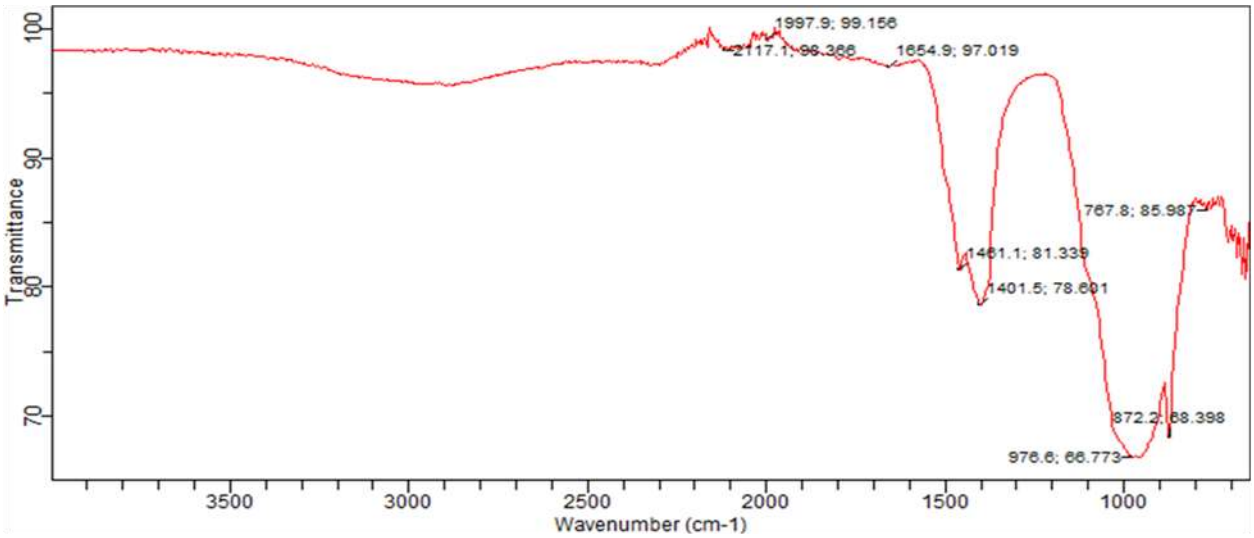

Fig. 2: Fourier Transform Infrared Spectroscopy (FTIR) of Musa paradisiaca Stalk Ash (MSA)

Figures 2 and Tables 2 show the spectra of the Musa paradisiaca Stalk Ash (MSA) used as coagulants was also measured in the range of 4000 cm^{-1} to 650 cm1 wave number. The peaks obtained at 2117.1 cm^{-1} corresponds to C≡C alkyne which indicates the presences of cyanide and thiocyanate ion, the peak at 1997.9 cm^{-1} corresponds to isothiocyanate (-NCS) and was due to transition metal carbonyls, the band at 1654.9 cm^{-1} is due to alkenyl C=C stretch suggests proteins or polyphenolic carbonyls, which can aid charge neutralization in coagulation, the band obtained at 1461.1 cm^{-1} corresponds to methyl C-H asymmetric/symmetric bend which indicates the presences of carbonate ions, the peak obtained at 1401.5 cm^{-1} is ascribed to O-H bend which indicates presences of phenol or tertiary alcohol, symmetric stretching vibration of COO-group of fatty acids and amino acids. CH_3 of proteins, symmetric bending modes of methyl groups in skeletal proteins, CH_3 of collagen important for particle binding and floc formation, the band obtained at 967.8 cm^{-1} indicates skeletal C-C vibrations and C-H Mon substitution (phenyl) and aliphatic fluoro compounds C-F stretch, the band obtained at 976.6 cm^{-1} corresponds to aromatic C-H plane bend which indicates the presences of silicate ion may add adsorption sites for contaminates , while the band obtained at 872.2 cm^{-1} also indicates aromatic C-H plane bend and presences of aromatic phosphate (P-O-C stretch) (Akinyemi, *et al*., 2020; Venegas, *et al*., 2022). These functional groups contribute to coagulation by bridging (Long-chain polysaccharides link suspended particles into flocs), electrostatic interactions (COO- groups binding positively charged particles and adsorption (phenolics/aromatics can adsorb organic pollutants and metals).

Table 2: Fourier Transform Infrared Spectroscopy (FTIR) of Musa paradisiaca Stuck Ash (MSA).

S/N	Peaks (cm^{-1})	Functional group
1	2117.1	C-=C ALKYNE
2	1997.9	ISOTHIOCYANATE (-NCS)
3	1654.9	Alkenyl C=C stretch
4	1461.1	Methyl C-H asym./sym. Bend
5	1401.5	phenol or tertiary alcohol, OH bend
6	767.8	Skeletal C-C Vibrations
7	976.6	Aromatic C-H in plane bend
8	872.2	Aromatic C-H in plane bend

3.1.2 Morphological Properties of *Musa paradisiaca* Leaf Ash (MLA).

Scanning electron microscope of *Musa paradisiaca* leaf ash (MLA)

Plates 1 shows the morphology behaviors of *Musa paradisiaca* Leaf Ash (MLA). These plates revealed that *Musa paradisiaca* Leaf Ash (MLA) has an irregular, porous surface and different sizes of cavities (Hussain, Hathout, Abdel-Mobdy, Rashed, Rahim and Fouzy, 2023; Ogunsuyi and Olawale, 2021). The SEM image of *Musa Paradisiaca* shows

a rough, porous and aggregated structure that is highly effective for coagulation. Its surface morphology supports adsorption, charge neutralization, bridging and sweep flocculation, making it a promising natural coagulant for water treatment.

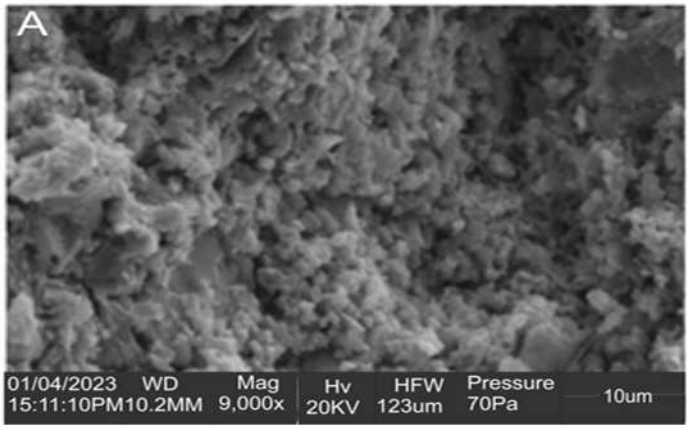

Plates 1: SEM of *Musa paradisiaca* Leaf Ash (MLA)

The energy Dispersice X-ray EDX is an analytical technique used for elemental composition measurements and chemical characterization of *Musa paradisiaca* Leaf Ash (MLA) (Ngankam, Dai-Yang, Debina, Bacaoui, Yaacoubi and Rahman, 2020; Utama, Sulistiyanto, Haidar, Barus, Haikal, Nugraha *et a*l., 2022).

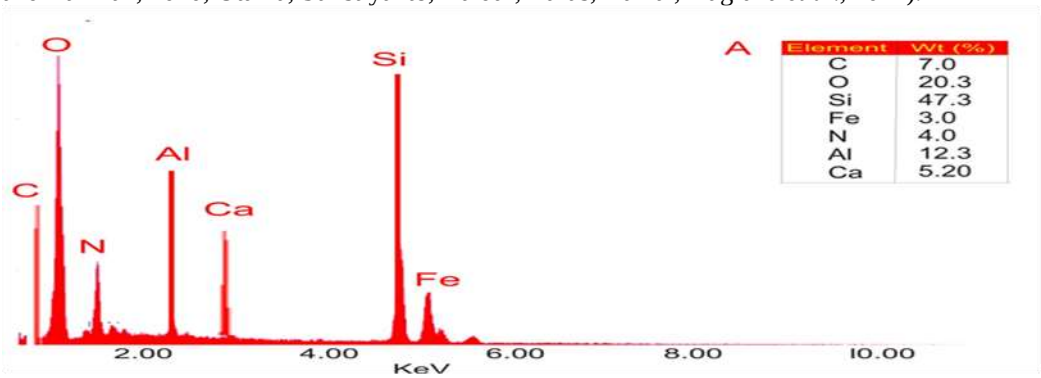

Figures 3: Energy Dispersice X-ray EDX of Musa paradisiaca Leaf Ash (MLA)

Figures 3 reveals existence of Aluminium (AI) 12.3%, Carbon (C) 7.0%, Calcium (Ca) 5.20%, Iron, (Fe) 3.0%, Nitrogen (N) 4.0%, Oxygen (O) 20.3% and Silicon (Si) 47.3%. The results of element concentration shows that *Musa paradisiaca* Leaf Ash (MLA) contains a high percentage of Oxygen and Silicon (Si). The high percentages of oxygen can be ascribed to derivates presence of primary metabolites fiber, carbohydrate and protein in *Musa paradisiaca* Leaf Ash (Falowo, Ejidike, Lajide and Clayton, 2021; Kamsonlian, Suresh, Majumder and Chand, 2011; Oyeyinka and Afolayan, 2019; Zaini, Roslan, J, Saallahs, Munsu, Sulaiman, Pindi, 2020). The presence of carbon noticed signifies the central components of carbohydrates, Lipids, Protein including Phyto organic compounds, silicon is regarded as quasi-beneficial and non-essential and is generally accumulated more in monocots (Bhat *et al*, 2019) while iron, is in trace element functions in the synthesis process of chlorophyll (Oyeyinka and Afolyan, 2021; Yiannikourides and Latunde-Dada, 2019). The high Silicon (Si) and Aluminium (AI) content means *Musa paradisiaca* can mimic conventional coagulants like alum or OAC (Poly-aluminium chloride). The Calcium (Ca) and Iron (Fe) content improve flocculation efficiency, especially of turbidity. The organic-inorganic hybrid nature makes Musa paradisiaca a sustainable, multifunctional coagulant. This elemental composition demonstrates strong potential for charge neutralization, bridging and floc formation, confirming Musa Paradisaca effectiveness as a green alternative to chemical coagulants in water treatment.

Scanning electron microscope of *Musa paradisiaca* stalk ash (MLA)

Plates 2 shows the scanning electron microscope which reveals the morphology of *Musa paradisiaca* stalk Ash. It shows an irregular, porous surface and different sizes of cavities (Hussain, *et al*., 2023; Ogunsuyi and Olawale, 2021).

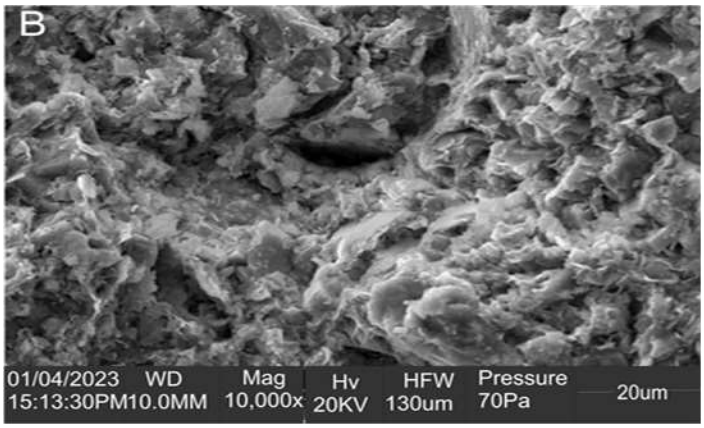

Plates 2: SEM of Musa paradisiaca Stalk Ash

The SEM image of Musa Paradisiaca shows a rough, porous and aggregated structure that is highly effective for coagulation. Its surface morphology supports adsorption, charge neutralization, bridging and sweep flocculation, making it a promising natural coagulant for water treatment.

Figures 6, represents the energy Dispersice X-ray EDX of a Musa paradisiaca Stalk Ash, it reveals the presences of Aluminium (AI) 7.5%, Carbon (C) 6.67%, Calcium (Ca) 22.09%, Iron, (Fe) 5.0%, Nitrogen (N) 4.0%, Oxygen (O) 10.43% and Silicon (Si) 44.31%. It was observed that silicon and calcium have the highest peak which can be attributed to high presences of silicon and calcium in Musa paradisiaca stalk. Calcium is important for optimal bone

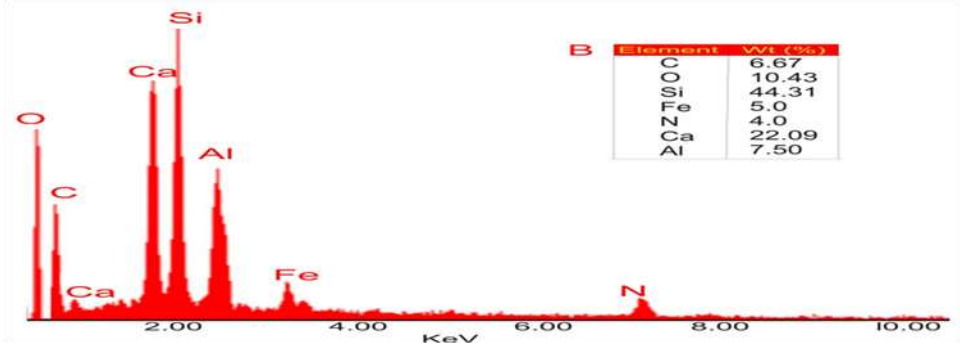

Figures 4: Energy Dispersice X-ray EDX of *Musa paradisiaca* Stalk Ash (MLA)

growth, development of heart, muscular and nervous system (Baryesi, Gallagher, McCarthy, Searles, Zhang, Link, *et al*., 2020; Narayanam, Chinni and Samuggam, 2021; Noirrit-Esclassan, Valera, Tremollieres, Arnal, Lenfrait and Fontaine *et al*., 2021; Oyeyinka and Afolayan, 2019). The EDX analysis shows that *Musa paradisiaca* samples contain significant inorganic elements (Si, AI, Ca, Fe) along with organic fractions (C, N). Sample a is AI-rich favoring charge neutralization while sample B is Ca- and Fe-rich favoring floc growth and sedimentation. Together these results confirm that *Musa paradisiaca* is a hybrid organic-inorganic natural coagulant, capable of both destabilizing colloids and promoting flocculation.

3.2 **Determination of anti-nutritional analysis**

The result of phyto-chemical or anti-nutritional analysis of Musa paradisiaca leaves and Stalk Ash are presented in Table 3. From the table 3 its shows that *Musa paradisiaca* leaf ash has 1.95 mg/100g, 0.16 mg/100g, 0.48 mg/100g, 8.7 mg/100g, 36.55 mg/100g, 18.6 mg/100g, 9.5 mg/100, 7.3 mg/100g, 54.4 mg/100g, 1.6 mg/100g and 8.6 mg/100g for tannin, phytate, alkaloid, saponin, flavonoid, crude protein, ash content, carbohydrate, crude lipids and crude fibre respectively while Musa paradisiaca Stalk Ash has 2.35 mg/100g, 0.19 mg/100g, 1.72 mg/100g, 2.7 mg/100g, 38.14 mg/100g, 2.1 mg/100g, 9.6 mg/100g, 9.2 mg/100g, 63.5 mg/100g, 0.9 mg/100g and 14.7 mg/100g for tannin, phytate, alkaloid, saponin, flavonoid crude protein, ash content, carbohydrate, crude lipids and crude fibre respectively. The observed variations in phytochemical concentrations between Musa paradisiaca leaf and stalk ash may be attributed to several factors, including differences in plant physiology, environmental conditions, and genetic variability. For instance, the higher alkaloid content observed in stalk ash (1.72 mg/100g) compared to leaf

Table 3: Anti-Nutrition Analysis

	Musa paradisiaca Leaf Ash	*Musa paradisiaca* Stalk Ash
Tannin	1.95	2.35
Phytate	0.16	0.19
Alkaloid	0.48	1.72
Saponin	8.7	2.7
Flavonoid	36.55	38.14
Crude Protein	18.6	2.1
Moisture Content	9.5	9.6
Ash Content	7.3	9.2
Carbohydrate	54.4	63.5
Crude Lipids	1.6	0.9
Crude Fibre	8.6	14.7

ash (0.48 mg/100g) may reflect tissue-specific accumulation patterns or differential expression of biosynthetic pathways. Similarly, the elevated crude fiber content in stalk ash aligns with the structural composition of stalk tissue, which typically contains a higher proportion of lignified cell walls and fibrous components. The presence of tannins in both leaf and stalk ash suggests potential antioxidant and antimicrobial properties, although their concentration may influence their bioavailability and bioactivity. Phytates, while possessing antioxidant properties, can also act as antinutritional factors by chelating essential minerals, thereby reducing their absorption. Alkaloids, known for their diverse pharmacological activities, exhibit varying concentrations in both ash types, indicating their potential contribution to the medicinal properties of Musa paradisiaca. Saponins, characterized by their amphipathic nature, may contribute to the emulsifying and foaming properties of the ash, with the leaf ash exhibiting a higher concentration compared to the stalk ash. Flavonoids, potent antioxidants with various health-promoting effects, are abundant in both leaf and stalk ash, suggesting their potential role in mitigating oxidative stress and inflammation

3.3 X-ray fluorescence of *Musa Paradisiaca* leaf ash and *Musa Paradisiaca* stalk ash.

The analysis of major and trace elements in geological materials by x-ray fluorescence (XRF) was made possible by the behaviors of atoms when they interact with radiation (Adeniyi, Ighalo and Onifade, 2019). Although FTIR analysis identifies the organic compound of the samples, the XRF identifies the natures of inorganic components present in the *Musa Paradisiaca* leaf/Stalk ash sample. Tables 4 presents the elemental components of Musa Paradisiaca leaf while Table 5 shows the elemental components of Musa Paradisiaca Stalk. From the X-ray Fluorescence of *Musa Paradisiaca* leaf ash presented in Table 4, silicon dioxide S_iO_2, iron (111) oxide Fe_2O_3, sulfur trioxide SO_3, calcium oxide C_aO, magnesium oxide m_gO,

Table 4: XRF Analysis of *Musa Paradisiaca* Leaf Ash

Component	Concentration (mg/cm^2)	Mole (%)
SiO_2	4.511	5.615
Fe_2O_3	2.346	1.099
SO_3	1.186	1.108
CaO	20.036	26.728
MgO	2.188	4.061
K_2O	55.786	44.299
Al_2O_3	4.06	2.979
Cl	5.584	11.781
SnO_2	2.656	1.318

potassium oxide K_2O, aluminium oxide Al_2O_3, chlorine Cl and tin (IV) oxide SnO_2 has a concentration of 4.511 mg/cm^2 , 2.346 mg/cm^2, 1.186 mg/cm^2, 20.036 mg/cm^2, 2.188 mg/cm^2, 55.786 mg/cm^2, 4.06 mg/cm^2, 5.584 mg/cm^2 and 2.656 mg/cm^2 respectively. The results of X-ray Fluorescence of *Musa Paradisiaca* leaf ash as presented are comparable with previous studies by Adenyi, Otoikhian, Onifade, Ighalo, (2019). From the X-ray Fluorescence of

Musa Paradisiaca stalk ash presented in Table 4, silicon dioxide S_iO_2, iron (111) oxide Fe_2O_3, phosphorus pentoxide P_2O_5, sulfur trioxide SO_3, calcium oxide C_aO, magnesium oxide m_gO, potassium oxide K_2O, aluminium oxide Al_2O_3, chlorine Cl and tin (IV) oxide SnO_2 has a concentration of 17.235 mg/cm^2 , 5.734 mg/cm^2, 3.052 mg/cm^2, 2.477 mg/cm^2, 30.955 mg/cm^2, 2.476 mg/cm^2, 27.702 mg/cm^2, 3.572 mg/cm^2, 3.564 mg/cm^2 and 1.91 mg/cm^2 respectively. The results of X-ray Fluorescence of *Musa Paradisiaca* stalk ash as presented are comparable with previous studies by Adenyi, *et al*., (2019). The *Musa Paradisiaca* stalk ash exhibits a higher concentration of silicon dioxide and calcium oxide compared to the *Musa Paradisiaca* leaf ash, which may reflect the structural requirements of the *Musa Paradisiaca* stalk tissue. The relatively high potassium oxide content in the *Musa Paradisiaca* stalk ash suggests that the *Musa Paradisiaca* stalk also plays a crucial role in potassium storage and translocation within the plant. The detection of phosphorus pentoxide indicates that the *Musa Paradisiaca* stalk contributes to phosphorus recycling, an essential element for energy transfer and nucleic acid synthesis. The differences in elemental composition between *Musa Paradisiaca* leaf and *Musa Paradisiaca* stalk ash highlight the functional specialization of these tissues in nutrient accumulation and distribution. The quantification of nutrients and minerals within various parts of a plant is important because it reveals the differences in requirements, accumulation and translocation of nutrients to various plant parts.

Table 5: XRF Analysis of *Musa Paradisiaca* Stalk Ash

Component	Concentration (mg/cm^2)	Mole (%)
SiO_2	17.235	19.845
Fe_2O_3	5.734	2.484
P_2O_5	3.052	1.487
SO_3	2.477	2.14
CaO	30.955	38.187
MgO	2.476	4.249
K_2O	27.702	20.345
Al_2O_3	3.572	2.423
Cl	3.564	6.954
SnO_2	1.91	0.877

Conclusions

Musa Paradisaca leaf ash phytochemical analysis shows strong potential as a natural coagulant for water treatment These findings underscore the compositional differences between the two ash types, indicating distinct biochemical profiles and potential functional attributes. The EDX analysis shows that *Musa paradisiaca* samples contain significant inorganic elements (Si, AI, Ca, Fe) along with organic fractions (C, N). favoring charge neutralization and floc growth and sedimentation. The scanning electron microscope of *Musa paradisiaca* leaf ash (MLA) and *Musa paradisiaca stalk ash* shows an irregular, porous surface and different sizes of cavities which supports adsorption, charge neutralization, bridging and sweep flocculation, making it a promising natural coagulant for water treatment. FTIR analysis confirms the role of hydroxyl, carbonyl and glycosidic groups in coagulation mechanisms. The results obtain in this research indicates the suitability of *Musa paradisiaca* leaf ash (MLA) and *Musa paradisiaca stalk ash* in water treatment applications.

References

Aborishade, A.B., Adetutu. A. and Owoade. A.O. 2017. Phytochemical and Proximate Analysis of some Medicinal Leaves. *Clinical Medicine Research*, 6(6), 209-214.

Ahamed, K.R., Chandrasekaran, T. and Kumar, A.A. 2013 Characterization of Activated Carbon Prepared from Albizia Lebbeck by Physical Activation. *International Journal of Interdisciplinary Research and Innovations*, 1(1), 26-31.

Akinyemi, O.P., Akinbomi, J.G. and Abbey, D.M. 2020. Comparative Characterization of Plantain Peel, Pawpaw Peel, and Watermelon Rind using FTIR. *Engineering and Technology Research Journal*, 5(1), 1-6.

Akpomie, K.G., Conradie, J., Adegoke, K.A., Oyedotun, K.O., Ighalo, J.O., Amaku, J.F., Olisah, C., Adeola, A.O and Iweozor, K.O. 2023. Adsorption Mechanism and Modeling of Radionuclides and Heavy Metals onto ZnO Nanoparticles: *A Review Applied Water Science*, 13(20), 1-24.

Aji, M. M., Gutti, B., and Highina, B.K. 2015. Production and characteristics of activated carbon from groundnut shell sourced in Maiduguri. *Columbian Journal of Life Science*, 17(1), 18-24.

Alprol, A. E., Mansour, A. T., Ibrahim, E. M., and Ashour, M. 2024. Artificial Intelligence Technologies Revolutionizing Wastewater Treatment: Current Trends and Future Prospective. Water, 16(2), 1-26.

Alsawy, T., Rashad, E., El-Qelish, M. and Mohammed, R.H. 2022. A Comprehensive Review on the Chemical Regeneration of Biochar Adsorbent for Sustainable Wastewater Treatment. Clean Water, 5(29), 1-21.

Arulpriya, P. and Lalitha, P. 2013. Determination of Proximate and Metabolite Composition of Aerial Roots of Rhaphidophora Area. (Linden Ex Andre) Twined over Two different Host Trees. *International Journal of Scientific Engineering. Research*, 4(12), 59-64.

Azman, A.S.N. and Adenan, D.S.A. 2019. Potential of Mangifera Indica seed as a Coagulant for Water Treatment. *Infrastructure University Kuala Lumpur Research Journal*, 7(1), 16-25.

Baryesi, R., Gallagher, M.J., McCarthy, L.A., Searles, E.K., Zhang, Q., Link, S. and Landes, C.F. 2020. Quantitative Analysis of Nanorod Aggregation and Morphology from Scanning Electron Micrographs using SEMseg. *American Chemical Society*, 124(25), 5262-5270.

Bhat, J.A., Shivaraj, S.M., Singh, P., Navadagi, D.B., Triparhi, D.K., Dash, P.K. and Deshmukh, R. 2019. Role of Silicon in Mitigation of Heavy Metal Stresses in Crop Plants. *Plants*, 8(3), 1-20.

Dada, A.O., Olalekan, A.P., Olatanya, A.M., and Dada, O. 2012. Langmuir, Freundlich, Temkin and Dubinin-Radushkevich isotherm studies of equilibrium sorption of Zn^{2+} unto phosphoric acid modified rice husk. *Journal of Applied Chemistry*, 3(1), 38-45.

Deng, R., Shao, R., Ren, B., Hou, B., Tang, Z. and Hursthouse, A. 2019. Adsorption of Antimony (111) onto Fe(111) Treated Humia Sludge Adsorbent Behaviour and Mechanism Insights Pollution. *Journal of Environmental Studies*, 28(2), 577-586.

Falowo, T.T., Ejidike, I.P., Lajide, L. and Clayton, H.S. 2021. Polyphenolic Content of Musa Acuminata and Musa Paradisiaca Bracts: *Chemical Composition, Antioxidant and Antimicrobial Potentials. Biomedical and Pharmocology Journal*, 14(4), 1767-1780.

Futi, A.P., Otieno, W.S., Acholla, O.J., Otieno, W.A., Ochieng, O.S. and Mukisira, M.C. 2011. Harvesting Surface-Rain Water Purification using Moringa Oleifera Seed Extracts and Aluminium Sulfate. *Journal of Agricultural Extension and Rural Development*, 3(6), 102-112.

Hirpa, L., Nigussie-Dechassa, R., Setega, G. and Bultosa, G. 2015. Chemical Quality of Common Beans as Influenced by Genotype and Aluminium Rates under Two Soil Liming Regimes. African Journal of Food, Agricultural, Nutritional and Development. 15(2), 9872-9891.

Hussain, O.A., Hathout, A.S., Abdel-Mobdy, Y.E., Rashed, E.A., Rahim, A. and Fouzy, A.S.M. 2023. Preparation and Characterization of Activated Carbon from Agricultural Waste and their Ability to Remove Chlorpyrifos from Water. *Toxicology Reports* 10, 146-154.

Karanja, A. Fengting, L. and Nganga, W. 2017. Use of Cactus Opuntia as a Natural Coagulants: Water Treatment in a Developing Countries. *International Journal of Advanced Research*, 5(3), 884-894

Iqbal, A., Hussain, G., Haydar, S. and Zahara, N. 2017. Use of New Local Plant based Coagulants for Turbid Water Treatment. International Journal of Environmental Science and Technology.

Jayalakshmi, G., Bhanya, K.D. and Saritha, V. 2016. Legitimate Use of Plant Waste Products for Drinking Water Treatment. *Journal of Environmental Research and Development*, 11(2), 351-359.

Jiang, L., Chen, Y., Wang, Y., Lv, J., Dai, P., Zhang, J., Huang, Y. and Lv, W. 2022. Contribution of Various Cd(11) Adsorption Mechanisms by Phragmites Australis- Activated Carbon Modified with Mannitol. *ACS Publications*, 7, 10502-10515.

Jiang, J.Q. 2015. The role of coagulation in water treatment. *Current Opinion in Chemical Engineering*, 8, 36-44.

Kamsonlian, S., Suresh, S., Majumder, C.B. and Chand, S. 2011. Characterization of Banana and Orange Peels. Biosorption Mechanism. *International Journal of Science Technology and Management*. 2(4), 1-7.

Karnena, M.K. and Saritha, V. 2022. Phytochemical and Physiochemical Screening of Plant-Based Materials as Coagulants for Turbidity Removal- An Unprecedented Approach. *Watershed Ecology and the Environment*, 4, 188-201.

Khader, E.H., Mohammed, T.H.J. and Mirghaffari, N. 2018. Use of Natural Coagulants for Removal of COD, Oil and Turbidity from produced Water in the Petroleum Industry. *Journal of Petroleum and Environmental Biotechnology*. 9(3), 1-7.

Kumar, R., Qureshi, M., Vishwakarma, D. K., Al-Ansari, N., Kuriqi, A., Elbeltagi, A., and Saraswat, A. 2022. A Review on Emerging Water Contaminants and the Application of Sustainable Removal Technologies Case Studies in Chemical and Environmental Engineering, 6, (100219) 1-14.

Kurniawan, S. B., Abdullah, S. R. S., Imron, M. F., Said, N. S. M., Ismail, N. Izzati, Hasan, H. A., Othman, A. A., and Purwanti, I. F. 2020. Challenges and Opportunities of Biocoagulant/Bioflocculant Application for Drinking Water and Wastewater Treatment and Its Potential for Sludge Recovery. *International Journal of Environmental Research and Public Health*, 17(24), 1-33.

Liang, S., Cao, S., Liu, C., Zeb, S., Cui, Y. and Sun, G. 2020. Heavy Metal Adsorption using Structurally Preorganized Adsorbent. *Royal Society of Chemistry*, 10, 7259-7264.

Lv, M., Zhang, Z., Zeng, J., Lui, J., Sun, M., Yadav, R.S. and Feng, Y. 2019 Roles of magnetic particles in magnetic seeding coagulation flocculation process for surface water treatment. *Sep. Purification. Technology*. 212, 337-343.

Mungondori, H.H., Muchingami, T.A., Taziwa, R.T. and Chaukura, N. 2021. Performance Intensification of the Coagulation Process in Drinking Water Treatment. *Water SA*. 47(2), 154-161.

Narayanam, H., Chinni, S.V. and Samuggam, S. 2021. The Impact of Micronutrients- Calcium, Vitamin D, Selenium, Zinc in Cardiovascular Health. A Mini Review. *Frontiers in Physiology*, 12(742425), 1-7.

Newman, D. and Cragg, G.M. 2020. Natural Products as Sources of New Drugs over the nearly Four Decades from 01/1981 to 09/2019. *Journal of Natural Products*. 83, 770-803.

Ngankam, E.S., Dai-yang, L., Debina, B., Bacaoui, A., Yaacoubi, A. and Rahman, A.N. 2020. Preparation and Characterization of Magnetic Banana Peels Biochar from Fenton Degradation of Methylene Blue. *Material Science and Applications*, 11, 382-400.

Noirrit-Esclassan, E., Valera, M., Tremollieres, F., Arnal, J., Lenfrait, F., Fontaine, C. and Vinel, A. 2021. *International Journal of Molecular Science*. 22(1568), 1-18.

Odika, I.M., Nwansiobi, C.G., Nwankwo, N.V., Ekwunife, C.M. and Onuoha, U.M. 2020. A Review on Treatment Efficiency of Pharmaceutical Effluents using Natural Coagulants. *International Journal of Environmental Chemistry*. 4(2), 54-61.

Ogunsuyi, H.O. and Olawale, C.A. 2021. Evaluation of Plantian Biomass (Musa Paradisiac L.) as Feedstock for Bio-Ethanol Production. *Scientific Research Publishing, Green and Sustainable Chemistry*, 11, 59-71.

Oluduro, A.O. and Aderiye, B.I. 2007. Impact of *Moringa Oleifera* Seed Extract on the Physiochemical Properties of Surface and Underground Water. *International Journal of Biological Chemistry*, 1(4), 244-249.

Oyeyinka, B.O. and Afolayan, A.J. 2021. Ultrastructure and Energy Dispersive Spectroscopy-Based Elemental Analysis of the Fruit Exocarps of Musa Sinensis L. (Banana) and Musa Paradisiaca L. (Plantain) (Musaceae). *Research Article*. 49(2), 1-9.

Oyeyinka, B.O. and Afolayan, A.J. 2019. Comparative Evaluation of the Nutritive, Mineral and Anti-nutritive Composition of *Musa Sinensis L*. (Banana) and *Musa Paradisiaca L*. (Plantain) Fruit Compartments. *Plants* 8(12), 598.

Peets, P., Kaupmees, K., Vahur, S. and Leito, I. 2019. Reflectance FT-IR Spectroscopy as a Viable Option for Textile Fiber Identification. *Heritage Science Journal*, 7(93), 1-10.

Peter, P.N., Robert, L.M., Mokgalaka, S.N. and McCrindle, R.I. 2011. Heavy metal Removal in Aqueous Systems using *Moringa Oleifera*. A review, *Journal of Materials Science and Engineering, B1*, 843-853.

Rahman, M.M., Ahmed, A.A.M., Khan, M.S.A. and Joy, S.S 2016. Performance Evaluation of Natural Coagulants (Cicer arietinum and Abelmoschus Esculentus) Comparing with Alum in Coagulation Process. *Proceeding of the 3rd International Conference on Civil Engineering for Sustainable Development*, 393-400. ISBN-978-984-34-0265-31.

Ratnaweera, H. 2020. Meeting Tomorrow's Challenges in Particle Separation with Coagulation. *In ACS symposium series*. 1348, 207-223.

Saravanan, J. Priyadharshini. D. Soundammal, A. Sudha, G. and Suriyakala, K. 2017. Wastewater Treatment using Natural Coagulants. *SSRG International Journal of Civil Engineering*, 4(3), 37-39.

Sasikala S. and Muthuraman G. 2017 Turbidity Removal from Surface Water by Natural Coagulants and its Potential Application. *Iranica Journal of Energy and Environment*, 8(1), 61-66.

Shan, Y. 2019. Evaluation of treatment efficiency of coal mine drainage and impact on surrounding waters for selected coal mines. IOP Conference Series Earth and Environmental Science, 349(1), 1-8.

Srinivasan, R. 2011. Advances in Application of Natural Clay and Its Composites in Removal of Biological, Organic, and Inorganic Contaminants from Drinking Water. *Advances in Materials Science and Engineering*, 2011, 1-17

Utama, C.S., Sulistiyanto, B., Haidar, M.F., Barus, O., Haikai, A.F., Nugraha, M.R.D., Sulistiono, S.D. and Bakhtiar, A.W. 2022. Scanning Electron Microscope Energy Dispersive X-Ray, Chemical, Organoleptic and

Microbiological Quality of Banana Peel (*Musa Paradisiaca L*.) at different Fermentation Durations. *Journal of Advanced Veterinary and Animal Research*, 9(3), 383-395.

Venegas, R., Torres, A., Rueda, A.M., Morales, M.A, Arias, M.J. and Porras, A. 2022. Development and Characterization of Plantain (Musa paradisiaca) Flour-Based Biopolymer Films Reinforced with Plantain Fibers. *Polymers*, 14(748), 1-15.

Venkata, M.P.S., Ramamohan, H. and Rao, B.S. 2017. Assessment of Coagulation Potential of Three Different Natural Coagulants in Water Treatment. *International Journal of Research and Scientific Innovation*, 4(12), 7-9.

Wang, Q. and Yang, Z. 2016. Industrial water pollution, water environment and health risks in China. Environment Pollution. 218, 358-365.

Wang, H., Wang, W., Zhou, S. and Gao, X. 2023. Adsorption Mechanism of Cr(Vi) on Woody-Activated Carbons, *Heliyon*, 9, 1-14.

Xu, Y., Qu, Y., Yang, Y., Qu, B., Shan, R., Yuan, H. and Sun, Y. 2022. Study on Efficient Adsorption Mechanism of Pb^{2+} by Magnetic Coconut Biochar. *International Journal of Molecular Science*, 23, 1-16.

Yang, X., Wan, Y., Zheng, Y., He, F., Yu, Z., Huang, J., Wang, H., Ok, Y.S., Jiang, Y. and Gao, B. 2019. Surface Functional Groups of Carbon-Based Adsorbents and Their Roles in the Removal of Heavy Metals from Aqueous Solutions: A Critical Review. *Chemical Engineering Journal,* 366, 608-621.

Yiannikourides, A. and Latunde-Dada, G.O. 2019. A Short Review of Iron Metabolism and Pathophysiology of Iron Disorders. Medicines. 6(85), 1-15.

Zaini, H.M., Roslan, J., Saallah, S., Munsu, E., Sulaiman, N.S., Pindi, W. 2022. Banana Peels as a Bioactive Ingredient and its Potential Application in the Food Industry. *Journal of Functional Foods,* 92, 1-12.

Zhao, Y., Xu, M., Lui, Q., Wang, Z., Zhao L and Chen Y 2018. Study of heavy metals pollution, ecological risk and sources apportionment in the surface water and sediments of the Jiangsu coastal region, China: A case study of the Sheyang Estuary. Mar. Pollut. Bull. 137,601–609.

Zhang, X. and Wu, N. 2022. Adsorption Characteristics of N-rGO for Multiple Representative Trace Antibiotics in Water. *Journal of Environmental Quality*, 51, 1298-1309.